1J-class Pulsed Plasma Thruster with Non-Volatile Propellant – Revisited

IEPC-2024-388

Presented at the 38th International Electric Propulsion Conference
Pierre Baudis Convention Center • Toulouse, France
June 23-28, 2024

Maciej Jakubczak[1], Arsenii Riazantsev[2], Olgierd Cichorek[3#], Agnieszka Jardin[4] and Jacek Kurzyna[5]
Institute of Plasma Physics and Laser Microfusion (IFPiLM), Hery 23, Warsaw, 01-497, Poland
[#]Space Research Center PAS, Bartycka 18a, Warsaw, 00-716, Poland

and

Przemysław Drożdż[6], Tomasz Palacz[7], Marcin Chuchla[8], Robert Łabuz[9] and Grzegorz Bywalec[10]
Liftero Sp. z o.o., Skotnicka 252A /4B, Cracow, 30-399, Poland

Abstract: In response to demands of the smallest satellites like CubeSats a breadboard model of 1 J-class ablative pulsed plasma thruster supplied with polymeric liquid nonvolatile propellant (PFPE) about 10 years ago was designed and evaluated. Despite sizing, the most rigoristic specification was power consumption limit, assumed to be 2 watts. The performance of the thruster when supplied with PFPE was estimated to be sufficient to provide a 1U CubeSat module with ΔV around 20 m/s from 2 g of the propellant consumed within 1 million firings. Aiming for such a thruster commercialization, its abilities were assessed again and compared with the performance of previous version. For new devices operated at 1 J the measured impulse bit appeared to be ~18 μNs, specific impulse ~400 s and efficiency ~3.5%. Two last quantities when reported for the previous project appeared to be 2.5-3 times greater than currently measured values. Some possible explanations for such large discrepancy are discussed.

I.Introduction

MICRO electric propulsion is currently offered commercially by several well established companies like Austrian Enpulsion, French Exotrail or Singaporean Aliena. The reliability of their products was confirmed in such missions as Flock 3P by Planet Labs (3U CubeSat), R2 by NanoAvionics (M6P 6U) and ORB-12 Strider by Orbital Astronautics (12U). However, there is still a need to develop and optimize thrusters fitting better to the demands and resources of the smallest satellites, even of pico class. Among several possibilities, an ablative pulsed plasma thruster[1] (APPT) fueled with polytetrafluoroethylene (PTFE – Teflon™), that builds on 70 years of

[1] Research Assistant, Department of Plasma Technology, maciej.jakubczak@ifpilm.pl
[2] Research Assistant, Department of Plasma Technology, arsenii.riazantsev@ifpilm.pl
[3] Research Assistant, Department of Plasma Technology, olgierd.cichorek@ifpilm.pl
[4] Research Fellow, Department of Plasma Technology, agnieszka.jardin@ifpilm.pl
[5] Research Fellow, Department of Plasma Technology, jacek.kurzyna@ifpilm.pl
[6] przemek@liftero.com
[7] tomasz@liftero.com
[8] marcin.chuchla@liftero.com
[9] robert.labuz@liftero.com
[10] grzegorz.bywalec@gmail.com

Copyright 2024 by the Electric Rocket Propulsion Society. All rights reserved.

experience in space, at the relevant dimensions might be a serious competitor for mentioned above (FEEP, Hall, resistojet) and other propulsive technologies.[2]

The great advantage of Teflon APPT structure is its simplicity. However, currently reported efficiency of miniaturized Teflon APPTs does not exceed 10% for the best optimized models when they are targeted to power range of just few watts.[3,4,5] Moreover, specific drawbacks like charring effect, late ablation or need to use separate Teflon blocks for each electrode pair in a multi-thruster systems able to provide 3-axial control stimulate searching for different propellants, also of liquid state.

Several years ago, for fueling 1 J-class APPT compatible with power available on-board of 1U CubeSat, perfluoropolyether (PFPE) was proposed as an alternative to PTFE.[6,7] Like all liquid fuels, PFPE might be distributed to several thrusters arranged in a system providing full mobility for a spacecraft, thus eliminating the problem of uneven use of propellant by individual engines. It was believed that some chemical similarity of this polymer to PTFE should grant thruster efficiency on par or better than that reported for Teflon (e.g. due to lowering the number of phase transitions). It was also expected that some PTFE drawbacks, like mentioned above charring effect, could be reduced or avoided. However, as far as managing of liquids in vacuum is concerned, the most attractive feature of this already space qualified fluid (as a lubricant) is very low vapor pressure which in room temperature may be of the order of 10^{-7} Pa, depending on the brand[8]. It means that this non-volatile liquid could be supplied to the discharge plenum well in advance before the ignition and wait for firing without evaporation as long as would be needed – in this way mimicking vacuum compatibility of solid propellants. It makes PFPE an unique among suggestions of other liquid fuels like water or alcohols which to be used in vacuum require a dedicated injecting systems[9] or other flow restricting solution like Scharleman's passive flow control method with porous materials[10].

Performance assessment of the first breadboard implementation of the 1 J-class APPT supplied with PFPE which had been designed within the frame of EC FP 7 project No. 283279 (*LμPPT – Innovative Liquid Micro Pulsed Plasma Thruster System for Nanosatellites*) appeared to be very optimistic, yielding impulse bit at the level of 15-20 μNs, specific impulse of 1000-1200 s, and thrust efficiency around 9.5%[7]. The reported numbers outperformed upper limit of the comparable Teflon APPTs which were available at that time. The next version of the micro APPT supplied with PFPE has been developed within the project *Pulsed plasma thruster for nano and micro satellites* funded by the Polish National Centre for Research and Development (NCBiR grant agreement No. POIR.01.01.01-00-0857/19), with the aim to improve the performance and provide a design ready for commercialization. The industrial leader of the project was Liftero Sp. z o.o. (formerly Progresja Space Sp. z o.o.) was responsible for fueling system, electronics, software and integration, whereas basic design of the thruster and its characterization were performed at IFPiLM. In this paper the performance assessment as well as results of lifetime tests of this new implementation will be presented. The paper organization is as follows. In Section II the thruster operation principle and some factors affecting its performance are presented. Next, the thruster implementation including fueling, powering and controlling systems is briefly described. Section III provides the information about the experiment arrangement with detailed description of the thrust stand specifics, measurement accuracy and the method applied for retrieving impulse bit. Finaly, in Section IV results of the thruster performance are presented and discussed in relevance to LμPPT project. The paper is closed with conclusions.

II. Thruster

Pulsed Plasma Thruster belongs to the class of electrodynamic accelerators in which thrust (impulse bit) is produced as reaction to abrupt blowout of ablated and ionized propellant, mostly caused by the Lorentz force $\boldsymbol{f}_L = \boldsymbol{j} \times \boldsymbol{B}$ which results from interaction of the discharge current density $\boldsymbol{j}$ with self-generated magnetic induction $\boldsymbol{B}$. The analogy to a rail gun[11,12] or pulsed plasma guns of different types has been suggested in literature[13].

Schematic of the thruster in the simplest rectangular configuration is depicted in Fig. 1. The thruster operates in vacuum. To maintain the discharge, concentric or flat (as in Fig. 1) electrodes are supplied with a battery of capacitors charged to a voltage of the order of 1 kV. This voltage is not sufficient to initiate an electric breakdown in the gap between the electrodes. For that, high voltage igniter (spark plug) is used which initiates low energetic flashover at the surface of the insulator that separates the electrodes[14]. The charged carriers

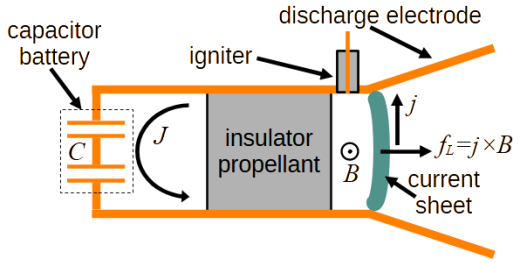

Figure 1. Schematic of Pulsed Plasma Thruster. The insulator/propellant block denotes solid PTFE or a system providing liquid propellant.

Copyright 2024 by the Electric Rocket Propulsion Society. All rights reserved.

produced in the flashover "short-circuit" battery that maintains current which, by energy transfer, ablates[15] the surface of the insulator. Due to subsequent ionization of released vapors the discharge current increases owing to positive feedback loop with the ablation process. Impulse bit I_{bit} produced by the thruster is a sum of electrodynamic I_{EM} and gas dynamic I_{GD} components: $I_{bit} = I_{EM} + I_{GD}$. Integration of $\boldsymbol{f}_L$ over the volume of plasma that carries discharge current J results in total electromagnetic force which in case of the thruster with parallel planar electrodes can be approximated[1] with formula $\boldsymbol{F}_L = \frac{1}{2}J^2\,\partial L$, from where $I_{EM} = \frac{1}{2}\partial L \int J^2 dt$ – here the integration is taken over discharge duration and ∂L denotes the thruster inductance derivative with respect to the coordinate along which plasma propagates (sometimes called in literature "inductance gradient", but incorrectly). Assuming isentropic expansion of ideal gas into vacuum, I_{GD} can be estimated[16] by formula $I_{GM} = (2/\kappa)\sqrt{2m_{bit}E(\kappa-1)/(1+\kappa)}$, where m_{bit} denotes gas mass released in the discharge, E amount of energy transferred to it, and κ heat capacity ratio. If m_{bit} is proportional to energy stored in the battery also I_{GD} becomes proportional to it[9]. According to the model of Mikellides et al.[17] gas dynamic term (for the thruster with parallel rectangular electrodes) is proportional to $\int J^{2/n} dt$ where n is propellant dependent constant (for Teflon $n = 0.8$). Thus, increase of both components of impulse bit requires growth of discharge current that can be done by increasing the energy stored in the battery and/or its inductance reduction. The battery and electrode system design was supported with numerical modeling (which will be discussed in the next paper) that allows for minimization of the thruster inductance for all sets of capacitors examined within the project.

A. Design considerations

Targeting 1U CubeSat with 1 J-class PPT we formulated the guidance to the design which included, among others, such factors like long term capacitor durability as well as energy storing density which govern the battery mass and volume. It was also assumed that the same battery construction should allow for thruster operation also with Teflon just by simple replacement of liquid fuel distributor with a block of solid propellant.

Table 1. Main characteristics of the optimized battery configurations for four different types of capacitors.

Battery type,	Mass, g	Capacity, μF	Inductance, nH	Lorentz force, μN
K-68	62	2.04	10.6	0.315
N-250	102	2.00	13.5	0.314
E-180	159	2.16	14.7	0.312
E-270	154	2.16	22.1	0.313

During implementation of LμPPT project it was found that of all the available ceramic capacitors the best energy packing factor offer ferroelectric ones. However, the battery built of them could withstand only about 50,000 shots of the thruster. Knowing that to provide Δv at the level of 20 m/s for a 1U module at least 1 million shots is needed, we searched for more reliable capacitors. Basing on robustness verified in series of dedicated tests, four types of ceramic chips (with C0G class as well as B2 and C4 type ceramic dielectrics) from different suppliers were selected. The construction of batteries for each type was similar. They consisted of two symmetric banks of capacitors between which dielectric distributor of PFPE was mounted. The banks were connected in parallel with copper brackets, in the middle of which convertible electrodes could be attached. The shape of brackets and orientation of capacitor chips resulted from the mentioned above modelling. Obtained initial inductance as well as relevant values of the Lorentz force at the surface of the insulators are summarized in Table 1 for all types of capacitors used in the experiments. It is interesting that despite significant span of the internal inductance the Lorentz force value at the surface of the insulator appeared almost the same for the optimized design. The differences in the inductance values are mostly caused by the volume of the capacitors which determines the size of the batteries and in this way the volume of the current loop.

Within modeling the impact of electrodes for the dynamics of the thruster inductance and the Lorentz force productions was examined as well. The electrodes are identified in literature as rectangular flat and tapered – both types can be parallel and flared[18]. Some most promising configurations (according to modelling) were examined experimentally within optimization tests for PFPE – see Section IV.

Copyright 2024 by the Electric Rocket Propulsion Society. All rights reserved.

a) b) 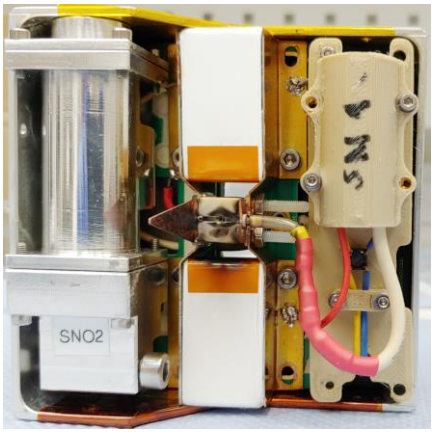

Figure 2. a) Two types of PFPE distributor: with the flat front surface and with deflectors of the expelled particles. At the left shown is attached connector of the feeding line. b) The thruster with N-250 battery as installed inside a case of CubeSat ½U module; fueling (at left) and igniting (at right) systems surround battery.

B. Assembling

One of the important goals of the current project was comparison of the LμPPT prototype yield with the current implementation performance. Generic construction of the thruster is prepared such that, depending on the needs, it can accommodate alternatively a block of PTFE or ceramic insulator (referred further as the propellant distributor) providing the thruster with liquid PFPE. For the latter purpose the insulator with the front surface of 1 cm × 1 cm is gouged with a groove in which the volume of PFPE of around 7 μl (that is sufficient for firing several hundred shots) could be contained. The groove connects both thruster electrodes in such a way that the open surface of PFPE is exposed to collisions with electrons emitted by a spark igniter. During thruster performance testing the groove was always oriented horizontally to avoid accumulation of PFPE in a privileged location due to the gravity. Two versions of fuel distributor tested within the current project are shown in Fig. 2a. The basic features of the distributor design resembles the solution invented within implementation of LμPPT project[7]. In the current design of the thruster assembly however, not only advanced fueling system supplying the groove (propellant plenum), but also different type and configuration of capacitors which build the energy storage bank as well as new charging and controlling systems are provided. The ready for testing thruster installed inside the ½U CubeSat module is shown in Fig. 2b. The basic parameters that affect the thruster dimensions and power consumption are kept as in the previous project, i.e. nominal discharge voltage is set to 1000 V, stored energy to 1 J and minimal thruster shot-to-shot repetition time to 1 s. The last value is governed by the power available on board of 1U CubeSat (which is assumed here to be around 2 W) and in case of bigger resources could be easily decreased.

Exemplary photos of discharge maintained at the surface of both propellants with K-68/2.16 μF battery are shown in Fig. 3. CCD camera was operated in an open shutter mode and images were taken in the whole optical range.

a) 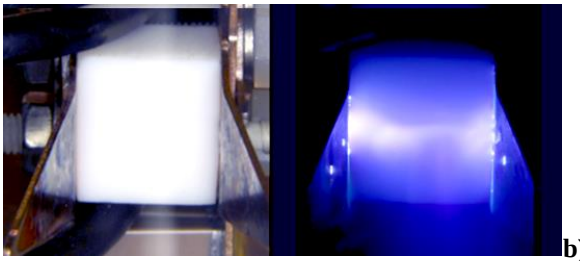 b) 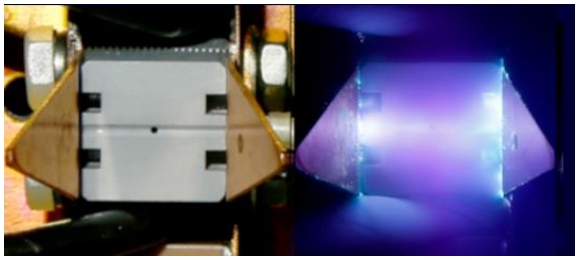

Figure 3. Discharge at the surface of PTFE – a), and along PFPE filling the groove in the insulator – b). Photos as taken with open shutter CCD camera in the whole optical range. (K-68 battery, discharge voltage 1 kV, igniter and the cathode at the right hand side of the thruster).

Copyright 2024 by the Electric Rocket Propulsion Society. All rights reserved.

C. Propellant feeding system

The propellant feed system should provide a precise dosage of propellant to the discharge block's groove over a wide temperature range and the resulting fluid viscosity change. It should be characterized by a simple construction, compact size, and high reliability. The maximum operational pressure of the tank should not exceed 6.9 bar to simplify the propulsion system's qualification process[19].

A fast-acting miniature valve is selected, and the flow model is incorporated to ensure the pressure and viscosity change compensation. A built-in transducer provides pressure and temperature measurements. Operating the tank in blow-down mode eliminates the need for pressure regulators. The system utilizes COTS (commercial-off-the-shelf) components and elements that can be manufactured relatively easily on a small scale. The system diagram is shown in the Fig. 4

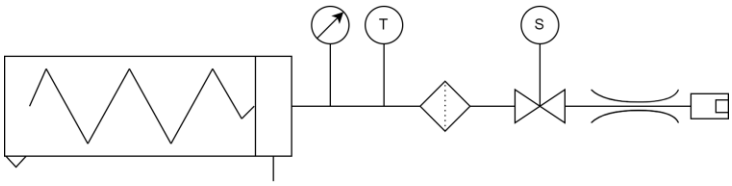

Figure 4. Propellant feed system diagram (from left to right): spring-loaded cylinder, pressure and temperature transducer, filter, solenoid valve, flow restrictor, discharge block.

Figure 5. Metal bellow tank flange.

Two implementations of the pressurized propellant tank were considered: one based on actuation through compressed metal bellow, the other - utilizing a piston with a compression spring. The first solution is characterized by greater simplicity (a single actuator element – metal bellow, as opposed to multiple components - piston, rings, and spring), higher reliability (sealing achieved by welding the bellow to the flange versus sealing with rings), and more stable operation (expansion of the bellow versus motion of the piston and rings along the cylinder surface). From a manufacturing perspective, the bellow-based solution is significantly more time-consuming and expensive for small-scale production. Ordering a custom component was not feasible within the project's timeframe and would have been very costly. Despite promising initial results conducted with a standard-size element (that would not fit the limited space available in the assembly), further development of this prototype (as shown in Fig. 5) was abandoned. The feed-system engineering model (depicted in Fig. 6) features a cylinder tank, a piston with two aerospace-grade low-friction guide rings, and one seal ring with a sliding ring. The spring compartment of the cylinder has a vent port allowing proper depressurization during ascent. The transducer / valve manifold attaches directly to the tank body. A mesh filter is integrated into the aforementioned manifold. A flow restrictor is connected to the manifold body via compression ring fitting.

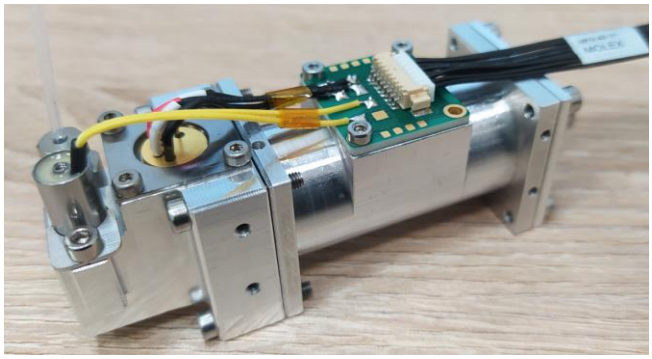

Figure 6. Feed-system engineering model.

With the selected flow restrictor and the designed pressure operation range of the propellant tank, it was possible to deliver a sufficiently precise and repeatable dose of propellant within the required operation temperature range. The performance test was conducted for two sets of parameters. The first set consisted of max. operating pressure in the propellant tank (tank at 100%), max. allowable operating temperature (lowest propellant viscosity) which resulted in the highest flow rate / fastest valve operation. The second set assumed minimal operating pressure (tank almost empty), minimal allowable operating temperature (highest propellant viscosity) which resulted in the lowest flow rate / slow valve operation (long hold operation). In both cases the selected miniature solenoid valve performed satisfactorily – delivering 89.7 mg and 81.41 mg of propellant on average per 100 dosing cycles. The open cycle time varied drastically – 14 ms in the first case and 16 s in the second case – to compensate for the significant change in the fluid's viscosity.

Copyright 2024 by the Electric Rocket Propulsion Society. All rights reserved.

The built-in compensation model was based on the empirical data from controlled environment tests (pressure, temperature, set valve open time). This model estimates the valve's open cycle time needed to deliver the requested mass of propellant, given current conditions (temperature, propellant tank pressure).

During the flow study, it was observed that dissolved gases in the propellant fluid significantly affected the valve's operation and the mass dispensed. In the case of operation in a vacuum environment, even the smallest amount of gas released caused liquid to be expelled from the capillary leading to overflowing the discharge block. Proper outgassing constitutes a major challenge for propellant loading and feed system handling, and operation. The support equipment developed in the project allowed the feed system to be filled under vacuum conditions. The process was preceded by several hours of heating and outgassing of the empty unit, simultaneously outgassing the propellant in a separate vessel. The fuel system was then gradually filled, still under high vacuum conditions (~10^{-6} mbar).

D. Thruster powering and controlling system

The electronic control unit (ECU) was designed from the ground up to achieve all necessary functionalities in a very low volume. The goal was to maintain a form factor of 0.5U for the entire thruster module. Another constraint was a low level of average power consumption, below 2 W, which necessitated focusing on the efficiency of voltage transformers. The unit must be capable of operating in a vacuum condition and able to conduct up to 1 million cycles to achieve sufficient total impulse.

The ECU consists of a few major functional blocks: the main battery charging unit, the high voltage ignition trigger unit, and the microcontroller-based control unit. During the hardware development stage, a strategy of modular construction was adopted. This approach was intended to allow for the independent development of basic functional blocks and their replacement if necessary. After the test campaign, a single-PCB architecture was implemented to achieve the desired size – see Fig. 7.

Figure 7. Assembled ECU module.

The main battery charging unit was designed to provide a voltage in the range of 500-1500 volts, supplied with 12 volts. The QR Fly-back architecture is widely used in power supplies and chargers with power up to 100W. Its main drawback is the high value of *dI/dt* during the commutation of the main switch from conduction to the blocking state. This characteristic potentially disqualifies this topology in this particular solution because the drive construction forces a large physical distance between the rectifier and the capacitors, resulting in significant parasitic inductance of this connection. However, during the course of the work, it turned out that in the boost configuration (output voltage greater than input voltage), parasitic capacitances play an important role. These capacitances occur both in the construction of the inductive element and due to the physical arrangement of the circuit components in the power supply construction, as well as significant inductance of the secondary winding. These capacitances, along with the inductance of the secondary winding of the transformer, form a resonant circuit that limits the values of *dU/dt*, enabling the power supply to operate despite the significant parasitic inductance between the rectifier and the capacitor bank.

The proposed design has shown: a) An ability to operate at a frequency of 1 Hz with battery energy >1 J. b) Capability to charge the capacitor bank to a voltage range from 500 to 1500V. c) Under operating conditions of 1 J/1 Hz, the electronic circuit consumes less than 2 W (average power) for both 2 µF and 1.5 µF capacitors – see Fig 8. Overall, the efficiency of the charging unit was 80%.

Copyright 2024 by the Electric Rocket Propulsion Society. All rights reserved.

The high voltage ignition trigger module was designed as a standalone converter providing voltages in the range of 200 – 250V. This converter powers a battery of ceramic capacitors with a capacitance of approximately 1 µF, working in conjunction with a high-voltage transformer. The discharge is initiated using an IGBT switch.

The SEPIC topology was chosen for the module, whose main advantages are a) Limited input current ripple. b) No overvoltage on the control switch during commutation. c) No direct current connection between the input and output of the converter. The last feature is extremely important because the output of the converter is shorted by the low resistance of the transformer's primary side during discharge generation.

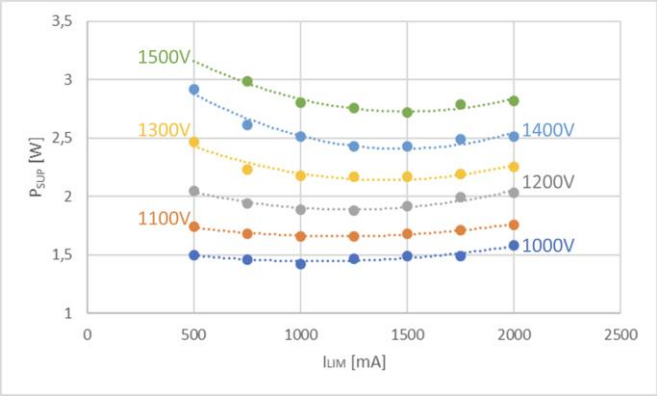

Figure 8. The average power of the PPT system for an operating frequency of 1 Hz, a capacitor bank with an electric capacitance of 1.5 µF, and a supply voltage of 12 V depends on the final voltage of the capacitor bank and the operating current.

In the control unit microcontroller used is the Microchip ATmega128, which, despite its simple 8-bit architecture, is sufficient for this application. In addition to the consumer version, it also has a high-reliability version and a version for space applications. The latter, in a plastic package variant, can be used without modifications to the existing design.

The clock signal source is an oscillator working with a quartz crystal. This part of the circuit proved to be particularly sensitive to interference generated by the spark gap, resulting in microcontroller hangs. The primary cause of the circuit's low interference immunity is the small amplitude of the signal in the quartz crystal circuit. Tests conducted using the internal RC oscillator showed improved device immunity to interference. Additionally, utilizing the "full rail-to-rail swing" mode available in the microcontroller, where the oscillator operates with a 3.3 V peak-peak output voltage, demonstrated that increasing the clock signal amplitude translates to system stability. However, both this solution and the earlier one with the RC oscillator are not feasible for the final implementation. The internal RC oscillator has too low frequency stability as a function of temperature, resulting in communication loss, while operating the quartz crystal with such a large signal amplitude significantly increases the component's failure rate.

The ECU comes with firmware that allows for autonomous propellant dosing and setting various testing parameters. The module connects to a PC using the MODBUS standard protocol over RS485. On the PC, a dedicated graphical user interface makes thruster control easy for the user.

III.Experimental Setup

All the tests towards thruster performance assessment were performed in the IFPiLM's electric propulsion laboratory – PlaNS. For impulse bit assessment the thruster was installed in a cylindrical vacuum chamber (with volume of ~2.5 m^3) at the thrust stand designed by Swiss MECARTEX company for the needs of the LµPPT project. The thrust stand will be described in some details in the next subsection. Testing was initiated only when the pressure inside this chamber was below 5×10^{-5} Pa (as measured with Ionivac Oerlikon-Leybold ITR 90 vacuum gauge). Owing to pump throughput of 2.8 m^3s^{-1} (TM Pfeiffer HiPace 3400 MC) and relatively long time (about 1 minute) needed for impulse bit measurement produced with a single shot, similar pressure was reproduced in the chamber before each subsequent

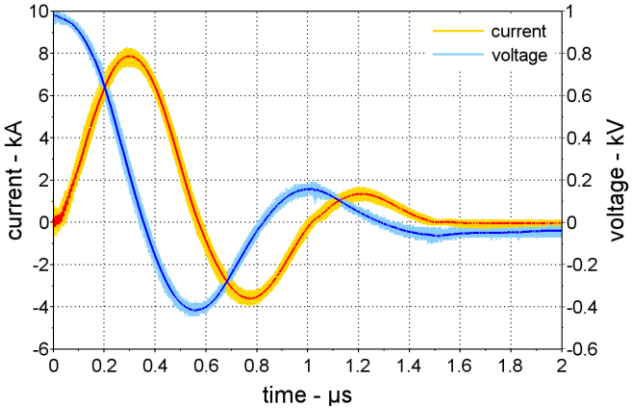

Figure 9. Mean discharge current and voltage averaged over 455 shots for E-180/1.98 µF battery supplied with PFPE. The curve backgrounds depict shot-to-shot repeatability.

Copyright 2024 by the Electric Rocket Propulsion Society. All rights reserved.

firing of the thruster. Auxiliary measurements needed for discharge *I-V* characteristics retrieving as well as mass bit assessment were carried out in a spherical chamber of 0.035 m^3 in which pressure during series of several hundred shots fired with frequency of 1 Hz did not increase above 2×10^{-4} Pa.
Having thruster battery assembled of two separate banks of capacitors, discharge current was retrieved by numerical summation of signals captured by two CWT 60B mini Rogowski coils with the dedicated integrators. Battery voltage was measured with high voltage Tektronix THDP0200 differential probe. All the signals were recorded with 8-bit Tektronix DPT5104 oscilloscope. Mean discharge voltage and current averaged over more than 450 shots are reproduced in Fig. 9 for the thruster with E-180/1.98 μF battery. The color backgrounds represent the range in which both characteristics are statistically scattered. Zero of time counting is arbitrarily set to the location in which current value at the increasing slope of each waveform is equal to 1% of the value of current in its first maximum.

A. Thrust stand and impulse bit measurement method

The impulse bit of the thruster was measured with mentioned above thrust stand (TS). In principle, it operates like a damped pendulum (to witch the thruster could be installed) suspended at a set of flexures with stiffness compensation. The displacement of the pendulum is proportional to the impulse of the force acting on it and can be recorded with high precision. Being designed for the needs of LμPPT project the sensitivity of this TB enables to measure impulse bit value at the level of single micro newton seconds. The TS was described in details in the previous papers[20,21] (in which it was used for Hall thruster performance assessment) and the reader is referred for technicalities to them. However, for the needs of the current project the TS had to be equipped with an external calibrator. The built-in one appeared not to be precise enough in the interesting range of the experimental conditions. Moreover, being also used as a damper of the pendulum oscillations, it could not serve for both purposes simultaneously. The new version builds on a current controlled voice-coil actuator**.** It can provide calibrated force in a range wide enough to be suitable for PPT as well as low power Hall thrusters. Due to the careful tuning procedure the mutual position of the magnet and the coil of the actuator were optimized to provide linear relation between voice coil current and the force produced in a wide range. That is illustrated in Fig.10

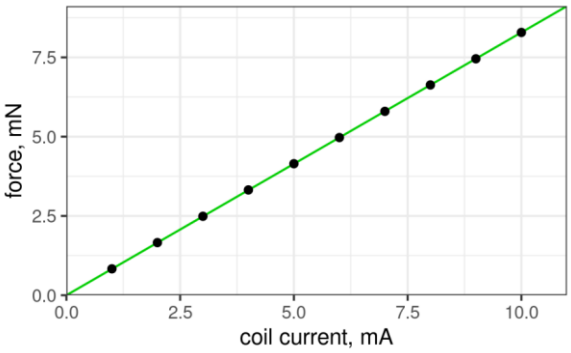

Figure 10. Relation between the force produced and the relevant coil current. Corresponding linear fit is depicted in green.

To check the TS displacement repeatability when the same calibrating force value is to be applied, a series of five subsequent switches on and off was triggered for two setpoints – see Fig. 11. The relevant displacement uncertainty was found to be 1% for 2 mN and 0.5% for 20 mN. The error analysis results in the combined standard uncertainty of the calibration force around 1.1%.

Oscillations of the TS pendulum can be described with the damped harmonic oscillator equation. Measurement of the impulse bit require retrieving the parameters (amplitude A, frequency ω and the mass m of the pendulum that includes the thruster) which fit the best to the oscillations of the TS recoded in the experiment. The relevant parameters must be recovered separately for the oscillations induced due to impulse bit production by the thruster and resulting from the switching of the calibrator.

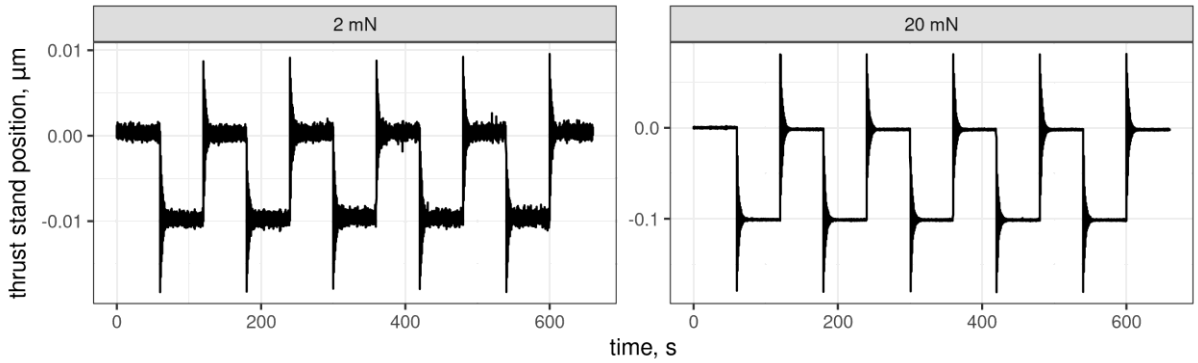

Figure 11. Records of repeatability tests for calibrator setpoint 2 mN (left) and 20 mN (right).

Copyright 2024 by the Electric Rocket Propulsion Society. All rights reserved.

Estimation of the amplitude A and frequency ω using the best fits for both signals allows for solving $I_{bit} = Am\omega$ formula for m if impulse bit is already known (like for the calibrator) and for I_{bit} (of the thruster) if mass m has been determined. The exemplary fitting of the TS oscillations induced by the thruster firing with the harmonic waveform is depicted in Fig.12 in green. With the trial-and-error method it was found that two initial oscillations after firing the thruster (or calibrator) provide the most reliable fits.

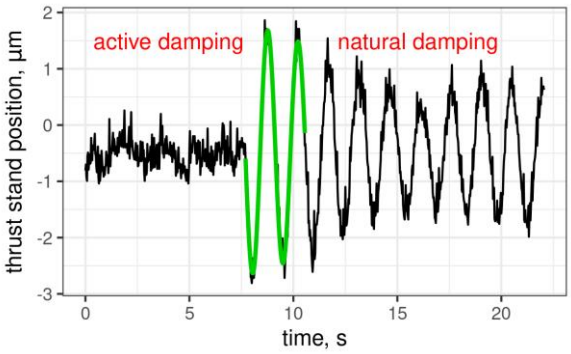

Figure 12. Typical record of TS signal used for the impulse bit measurement. Best fit with harmonic oscillations using two initial vibrations is shown in green.

The following procedure was applied during the measurements. First, TS equilibrium position was adjusted. To cancel natural vibration the TS active damper was used (operating as a PID regulator). Next, for recording of the signal useful for impulse bit measurement, the thruster was triggered as soon as the damper has been switched off by the operator. The same procedure was applied for the calibrator, but only once per setup modification (the mass change due to propellant consumption was negligible). For calibrator the impulse bit of desired magnitude was simulated by 1 ms current pulse of defined amplitude. Having both fits accomplished, all the needed parameters could be established and the thruster impulse bit determined. To estimate variance of the measurements the follow-up experiment was done using the calibrator as a trusted impulse bit source. The setpoint was chosen to agree with a value from the actual PPT yield. Total uncertainty of the mean impulse bit averaged over 50 values determined from the thruster shots has been estimated to be around 2%. The analysis showed that the main factor making this number is residual momentum of the pendulum at the moment the impulse bit is generated.

Assessment of the thruster efficiency and specific impulse requires measurement of mass bit m_{bit} per a shot (of the order of micro grams). For that, the total mass loss Δm of the propellant corresponding to the number N of shots fired within a series was determined by weighting the thruster or just the propellant block using an analytical balance. Weighting at the beginning and the end of the series results in $m_{bit} = \Delta m/N$. Two analytical balances OHAUS EX1103 and EX324 with maximum weight capacities of 1.1 kg and 0.32 kg and relevant readabilities 1.0 mg and 0.1 mg were used. To determine the usage of PFPE two procedures were applied. Within the first one the propellant distributor was fueled "by hand" and weighted with the more sensitive balance when disassembled from the thruster. However, here the additional source of errors appears due to uncontrolled PFPE loss during separation of the distributor. The second procedure was weighting the completely assembled thruster using the less sensitive balance. Beside obvious drop in accuracy the new source of errors is uncontrolled absorption and releasing of the atmospheric water by the elements of the thruster during its residence outside and inside the vacuum chamber. Bearing in mind the mentioned effects it is obvious that mass bit assessment accuracy has to be limited, no matter how restrictive routine for reducing residence time in atmosphere and to minimize interval between venting the chamber and weighting the thruster would be applied.

IV.Results and Discussion

Despite assessment of PTFE thruster is out of the scope of the current paper it is worth noting that we fired in total $\sum N = 1\,029\,220$ shots during relevant tests. Seeing no degradation in operation of the whole thruster as well as no visual signs of damage at the battery we decided that the lifetime test of 1 million shots has been passed. This results could be anticipated for PFPE as seems reasonable to assume that battery lifetime should not depend on the propellant but mostly on the robustness of capacitors.

A. Performance of the thruster supplied with liquid PFPE

To test the thruster supplied with PFPE propellant E-180/2.16 µF battery and two types of ceramic distributors able to provide liquid propellant were used – see Fig. 2. Searching for the optimal architecture of the thruster, we varied electrode configurations as well as switched between the distributors. For simplicity, configuration with 20 mm long, tapered electrodes flared at the angle of 15° with respect to the symmetry plane and the distributor with flat facial surface will be further referred to as basic one.

Despite the specifics of each thruster setup, all the tests were run along the same scheme. After opening the miniaturized electromagnetic valve of the fueling system the groove in the distributor was filled up with PFPE

Copyright 2024 by the Electric Rocket Propulsion Society. All rights reserved.

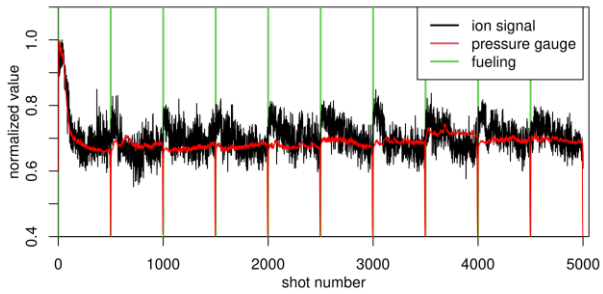

Figure 13. Sequence of RS cycles initiated after a long break. The first RS cycle always produced higher pressure variation in the vacuum chamber. Vertical lines separate cycles within a series.

owing to pressure induced inside the fuel tank by a piston system (see Subsection C of Section II). The volume of the groove was sufficient to provide fuel for several hundred to around thousand shots, depending on the discharge voltage (energy stored in the battery). Both phases: groove filling and the thruster firing until fuel depletion, will be further referred to in common as filling-firing (FF) cycle. The dose of PFPE as well as other parameters like number of shots until the next groove refilling, charging voltage and discharge repetition frequency were controlled with a dedicated application operated from the laboratory computer. For impulse bit measurements the thruster was installed at the TS inside the bigger chamber. The actual measurements were always preceded with at least four FF preparatory cycles performed for stabilization of the thruster operation. The similarity of subsequent FF cycles is illustrated in Fig. 13 in which variations of the pressure inside the chamber and the ion collector current as measured at the axis of the expelled plasma plume are shown. Except for the first one or two initial cycles, the next ones appeared to be satisfactorily repeatable. Stronger signals visible in the initial FF cycles within series were mostly the result of the growth of a propellant surface exposed to the discharge due to PFPE creeping in vicinity of the groove during a long interval between subsequent measurement series (e.g. night or weekend). The number of shots within each FF cycle performed during each measurement series was always kept constant. For that, the propellant dosage appropriate for the given battery voltage was established first by the trial-and-error method.

The character of ion current suggests that mass released per shot varies within the FF cycle (mostly due to propellant consumption). That may result in similar impulse bit variations. Indeed, it was confirmed by the direct measurements with the TS: soon after the start of a FF cycle, I_{bit} gained the maximum value, whereas moving towards the cycle end I_{bit} asymptotically decreased to a constant value. To figure out statistically meaningful numbers, the measured values were averaged twice: first over 10 subsequent shots within the FF cycle (to smooth shot-to-shot scattering) and next over 3 subsequent FF cycles (to smooth over the series). The number ten was chosen as significantly smaller than the FF cycle length (about 500 for battery energy of 1 J), but yet reasonable for averaging. The number of ignored firings preceding any ten firings of interest was varied along the FF cycle

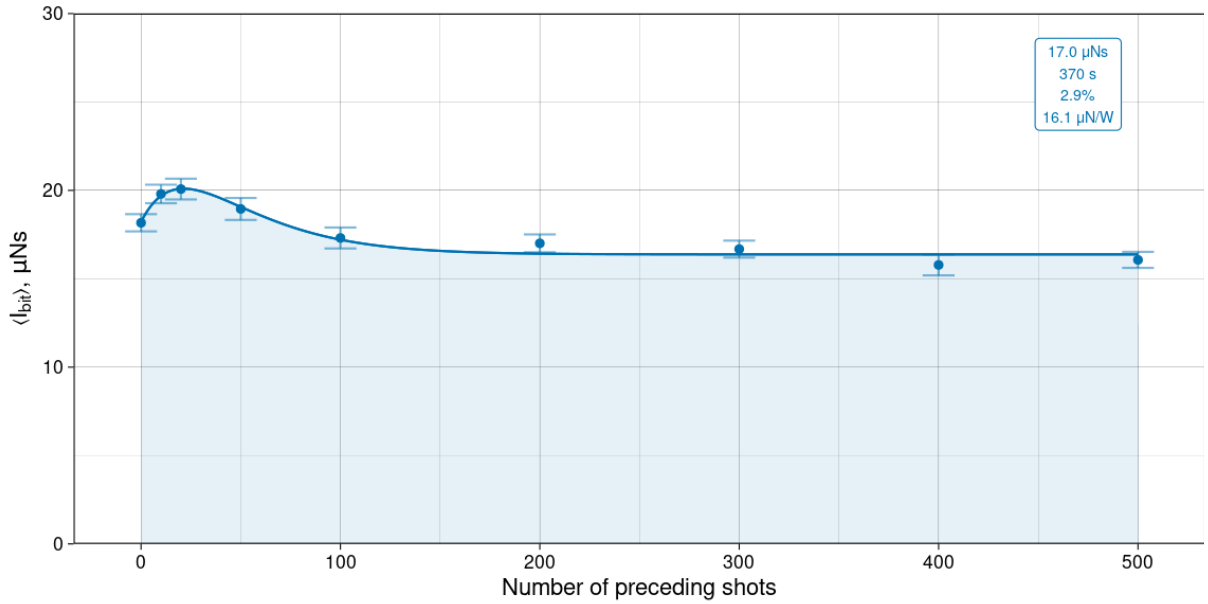

Figure 14. Impulse bit as averaged over 3×10 shots vs preceding shot number. Numbers in box (from top to bottom) are mean values of the thruster impulse bit, specific impulse, energetic efficiency and thrust to power ratio.

Copyright 2024 by the Electric Rocket Propulsion Society. All rights reserved.

according to the rate of I_{bit} dynamics. Having the pattern already established, it was applied unchanged for the next two FF cycles taken for the mean value calculation. In this way evolution of the impulse bit mean value within FF cycle was retrieved using averaging over 3x10=30 data points for several strictly defined shot indices.

The evolution of mean impulse bit value along FF cycle as calculated according to the procedure described above is depicted in Fig. 14 for the basic thruster configuration. The curves shown are parametrized with energy stored in the battery. They can be approximated with function $f(x) = Axe^{-Bx} + Cx + D$ which was used for analytical integration needed to calculate mean impulse bit of the thruster, defined as $\overline{I_{bit}} = \int f(x)dx/N_{FF}$ where integral is taken over all N_{FF} shots within relevant FF cycle.

Calculations of specific impulse $I_{sp} = I_{bit}/m_{bit}g$ and energetic efficiency $\eta = I_{bit}^2/2m_{bit}E$, require knowledge of mass bit value (here E denotes energy stored in the battery, and g the standard Earth's gravity). For that, the thruster was weighted before and after a series of shots and the resulting mass difference was divided by the number of firings. To increase accuracy of mass bit measurements, the number of shots in the current tests was set to 10000 and the more sensitive analytical balance was used. However, to avoid the balance overloading and simultaneously uncontrolled loss of the propellant, the thruster had to be dismantled in such a way as to allow for weighting the fueling system and the battery assembly still connected together. The procedure appeared effective and less biased results were obtained than in the case of LµPPT, where only limited number of shots with liquid propellant could be fired. The mass bit uncertainty was estimated conservatively to be 10%.

Performance of the basic configuration is illustrated in Fig. 14. The results of the tests immediately show significantly worse performance of this implementation of the thruster compared to LµPPT. To regain high efficiency, other configurations were subsequently tested.

1. Flare angle optimization

Searching for the better thruster configuration, first, the impact of the electrode divergence was examined. For that, the electrodes of the basic configuration were replaced with two pairs of 2 cm long tapered blades with relevant flare angles of 22.5° or 30°. The results are summarized with plots and legends presented in Fig. 15. To make the comparison easier, the results for the basic configuration are also depicted there. In this experiment mass bit needed for performance assessment was not measured, but taken the same as for the basic configuration – it was assumed that the ablation yield depends mainly on the initial phase of the discharge, when it is attached to the propellant surface. In this region geometry of the electrodes was independent of the flare angle and mass bits should be similar to the previously measured ones. There is no reason to suspect that assumption is not valid and could affect the outcomes, because the same number of shots was actually fired within one FF cycle for basic and other

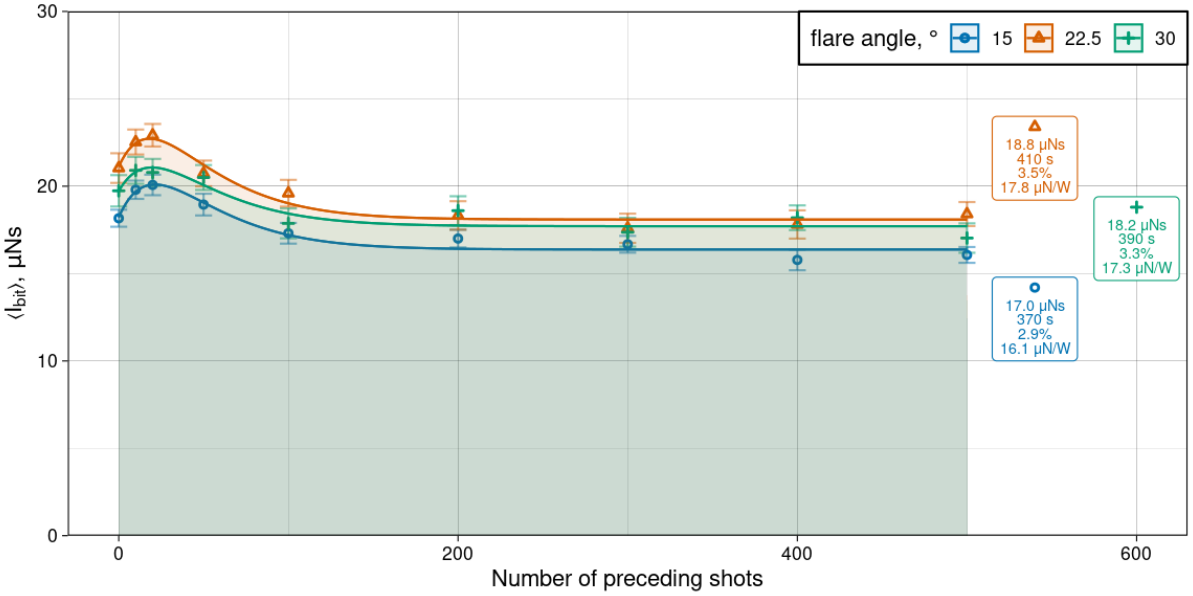

Figure 15. Impulse bit as averaged over 3×10 shots vs preceding shot number. Different flare angles are distinguished with colors and symbols. Numbers in relevant boxes (from top to bottom) are mean values of the thruster impulse bit, specific impulse, energetic efficiency and thrust to power ratio.

Copyright 2024 by the Electric Rocket Propulsion Society. All rights reserved.

configurations.

The obtained outcomes of the tests show that there is an optimum flare angle, resulting in the growth of the overall thruster performance with respect to the basic configuration. Although the difference between 22.5° and 30° is not huge, the results presented above suggest to use in the subsequent tests thrusters with electrodes inclined at the angle of 22.5°.

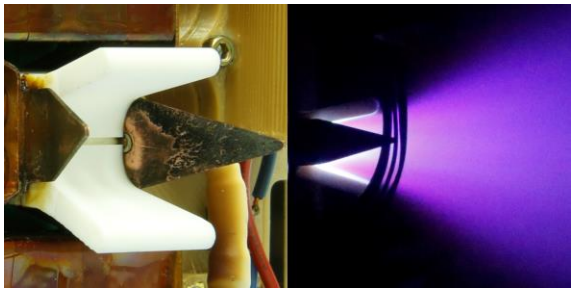

Figure 16. Distributor with flared deflectors (left) as installed between electrodes and plasma plume expelled during thruster operation (right).

2. Anticipating gas-kinetic effects

In this experiment the same pair of tapered electrodes (22.5° flared) as in the previous tests was used. However, PTFE distributor with flat facial surface was replaced by construction provided with two planar deflectors flared with respect to the thruster symmetry plane. It was expected that random movements of hot neutral particles would be directed towards the thruster axis increasing impulse bit production and finally improving mass and energy budget of the thruster. The phots of the thruster equipped with new distributor and operating in the vacuum chamber are reproduced in Fig. 16, whereas its performance is presented in Fig. 17.

Contrary to expectation however, it appeared that the modification slightly reduced thruster abilities.. It seems that the distributor deflectors obscured plasma plume geometrically resulting in loss of energetic particles able to produce impulse bit due to electrodynamical acceleration. In these circumstances the positive input to performance owing to gas-kinetic nozzle effect, if any, appeared to be lost. To exploit this effect, the distributor has to be redesigned towards construction able to operate simultaneously as a valuable gas nozzle and fuel providing device.

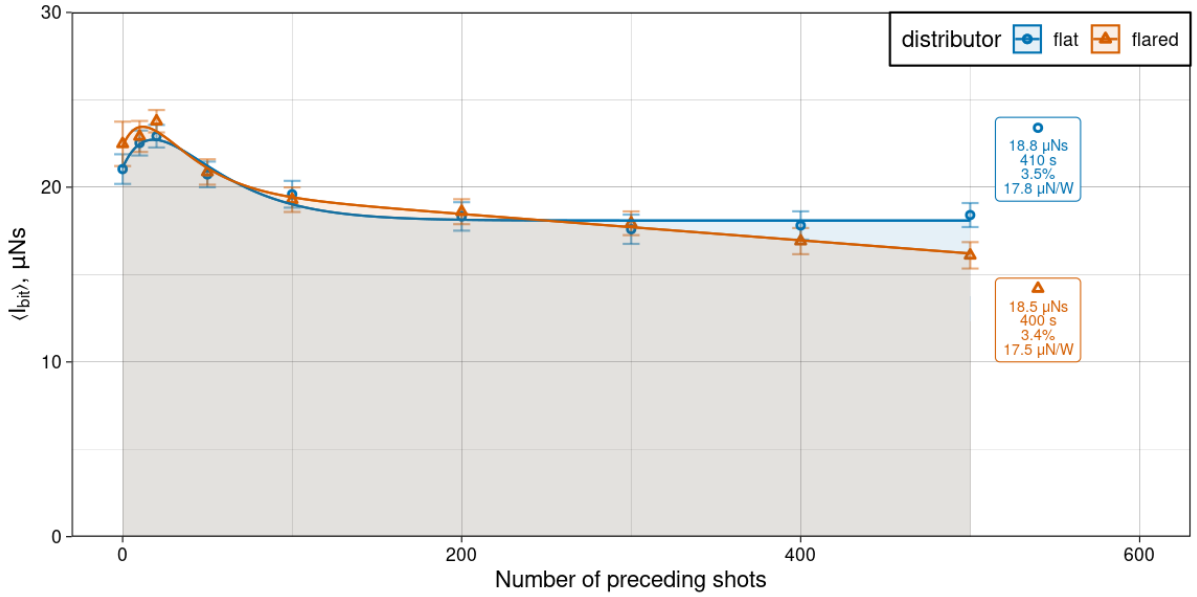

Figure. 17. Impulse bit as averaged over 3×10 shots vs preceding shot number. Different distributors are distinguished with colors and symbols. Numbers in relevant boxes (from top to bottom) are mean values of the thruster impulse bit, specific impulse, energetic efficiency and thrust to power ratio.

3. Alternative electrode configuration

As the last thruster configuration we examined the version which, according to numerical modelling, should provide the fastest inductance growth as well as the largest Lorentz force, that is the geometry labeled as "narrow" one. If the slug model is valid, plasma acceleration efficacy should increase resulting possibly in the thruster performance improvement. The narrow electrodes were 0.5 mm thick, 1.0 mm wide and 20 mm long, and flared at the angle of 22.5°, whereas the distributor was brought back to the standard one with flat facial surface – see Fig. 18.

Copyright 2024 by the Electric Rocket Propulsion Society. All rights reserved.

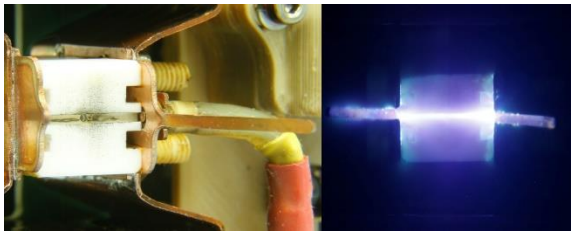

Figure 18. Thruster equipped with flared (22.5°) narrow electrodes (0.5 mm×1.0 mm×20 mm).

The test results are presented in Fig. 19. The unexpected outcome was significant decrease of the mass bit despite the electrodes arrangement in vicinity of the propellant plenum and the igniter was exactly the same as in the all remaining configurations with the same distributor. Thus, the shot number per one FF cycle increased from 500 to 800 (i.e. by 60%) with respect to the basic configuration. The most important impact on the overall thruster performance appeared as the increase of the specific impulse by around 24%, whereas efficiency increased only by 8.6%. Such big specific impulse growth mitigated impulse bit decrease (caused mainly by lower mass bit production), so that it finally drops only by ~14.5% (similarly to thrust-to-power ratio).

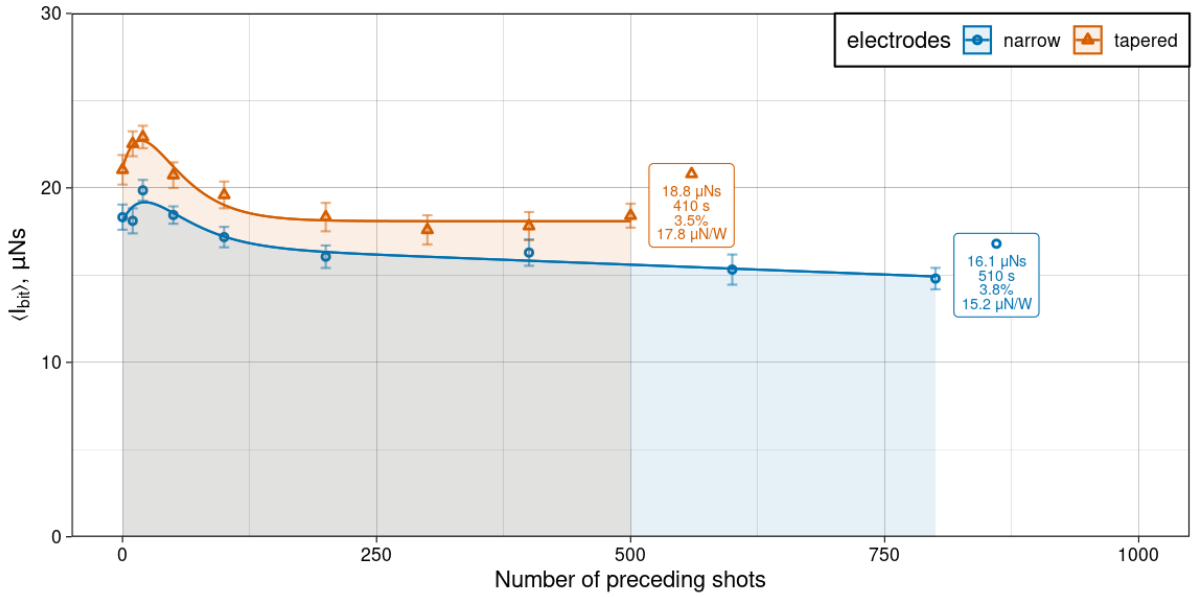

Figure 19. Impulse bit as averaged over 3×10 shots vs preceding shot number. Different electrode shapes are distinguished with colors and symbols. Flare angle was 22.5°. Numbers in relevant boxes (from top to bottom) are mean values of the thruster impulse bit, specific impulse, energetic efficiency and thrust to power ratio.

4. Results review

Results of tests accomplished for the thruster supplied with PFPE are recapitulated in Table 2. The uncertainty of impulse bit for PFPE is about 2% only due to good repeatability of the discharge. It seems that it is mainly caused by fixed choice of the discharge path at the surface of PFPE because of the propellant geometry limited to the narrow groove. It is confirmed with photos taken by open shutter camera like those reproduced in Fig. 3 and Fig. 18 as well as with fast photography which is presented in a separate paper[22]. This effect is reproduced by small scattering of data points and subsequently short error bars in Fig. 14.

Analyzing performance of different PFPE thruster configurations, it is worth noting that in relevance to tapered 22.5° flared setup, the narrow one offers 26% gain in I_{sp}, with concurent drop in I_{bit} by 13% (and obviously the thrust-to-power ratio). Simultaneous drop in mass bit by around 32% results in 8% increase in η, but this value remains within measurement uncerteinty, so one can conclude that both configurations provide similar energetic efficiencies. It is an open question why mass bit in this configuration is reduced – one of the possibilities is smaller plasma volume which results in less efficient interaction with propellant surface. Moreover, it may also suggest that significant ablation is supported during plasma expantion in configurations with wide electrodes that is not the case for the narrow ones and hence the narrow plasma. However, such explanation would be contradictory to exploited earlier assumption about equal mass production due to similarities of geometry in vicinity of the propellant surface.

Copyright 2024 by the Electric Rocket Propulsion Society. All rights reserved.

Table 2. Summary of the thruster performance with PFPE propellant

configuration	energy, J	mass bit, μg	I_{bit}, μNs	I_{sp}, s	efficiency, %
basic: 15° flared, tapered, distributor flat	1.056(32)	4.72(47)	16.96(26)	366(37)	2.88(31)
22.5°	1.056(32)*	4.72(47)*	18.79(36)	406(41)	3.54(39)
30°	1.056(32)*	4.72(47)*	18.24(39)	394(40)	3.34(38)
22.5° distributor flared	1.056(32)*	4.72(47)*	18.49(30)	399(40)	3.43(38)
22.5°, narrow, distributor flat	1.056(32)*	3.20(32)	16.10(32)	513(52)	3.83(43)

**values assumed relying on the basic configuration*

From the point of view of the mission mass budget, narrow configuration could be preferable, but more detailed studies are still necessary – this configuration was examined in one variant only.

The comparison of the PFPE thruster performances obtained during LμPPT project and the current one is not straightforward because for the same voltages relevant battery energies differ (for discussion of the voltage-energy relation for ferroelectric capacitors please see Ref. 7). Performance as measured within LμPPT project for thruster operated at 1.0 kV and 1.5 kV (but with two different batteries) is reproduced in Table 3. Very strong discrepancy of the results from both projects (that is clear even though the setpoints are not exactly the same) can be partially explained by inaccuracy of the TS built-in calibrator that was used previously. Precision of the new calibrator was confirmed in dedicated tests as described in Subsection A of Section III. Results of the checking measurements with the use of both calibrators reveals that outcomes of the previous TS measurements were overestimated by 30% (so that the true value of I_{bit} for 1 kV, 1 J case should have been 15.8 μNs – value even smaller than in the present implementation). Moreover, it seems that yet another serious source of the inconsistency stems from the mas bit measurements. In the previous project there was no automatic fueling system and consequently mass bit had to be determined relying on relatively low number of shots, that could result in its gross underestimation and hence overestimated values of the specific impulse and efficiency. Indeed, also within the current project, when the automatic fueling system was not ready yet, we supplied the groove with PTFE "by hand", that resulted in almost two times lower mass bit value than obtained from the automated measurements. Of course, additional hard to assess factor after the years is battery design itself, that affects time and amplitude characteristics of the discharge. Nevertheless, comparing discharge currents for 1 kV as measured in both projects one can notice that despite the relevant values in maxima are almost the same, the semi period of the LμPPT current was longer by 20-30% whereas damping stronger (please see current and voltage waveforms reported in Ref. 7). Such character of current dynamics could stem from bigger effective battery capacitance and also from derating of ferroelectric capacitors which were used in the previous project. Checking whether longer discharge duration could be indeed the reason of better thruster performance is left to the future experiments.

Table 3. Thruster performance as measured within LμPPT project.

battery	energy, J	mass bit, μg	I_{bit}, μNs	I_{sp}, s	efficiency, %
No. 1 - 1000 V	1.25	1.65	20.5	1240	10
No. 2 - 1500 V	1.56	2.4	26	1080	9

V.Conclusions

The optimization studies showed that performance of the PFPE system may be improved by shaping electrode configuration, that was supported with numerical modelling of the battery configuration. The gain in some

Copyright 2024 by the Electric Rocket Propulsion Society. All rights reserved.

parameters was as large as 30%-40% in relevance to the basic configuration. It is worth noting that very special configuration with narrow 22.5° flared electrodes provides I_{sp} greater by 26% than its tapered analogy. Only 13% drop in impulse bit with respect to relevant 32% drop in mass bit suggest more efficient acceleration in the narrow configuration Unfortunately, configuration optimization was not performed here for PTFE thruster and the direct comparison is now not possible. Nevertheless, comparing our PFPE thruster performance with optimized PTFE designs known from literature one can notice that the yield is on par – see e.g. Ref. 5 for 2 J PTFE thruster.

However, comparing performance of the thruster assessed within LμPPT project with the abilities of the current design, the discrepancy is puzzling. It can be partially explained by inaccurate calibration of the TS in the previous studies. It seems that another reason of the overestimated performance were unreliable mass bit measurements. In case mass bit measurements were after all correct, responsible for such high performance could be only different battery design (including type of capacitors) that should be verified with the separate studies.

Demonstrated here constructional solutions, fitting to energetics of 1U CubeSat module, battery lifetime proved to withstand 1 million shots as well as satisfactory performance confirm that the elaborated within the project thruster design is matured enough to propose commercialization.

Acknowledgments

The presented study was carried out as part of the project "Pulsed plasma thruster for nano and micro satellites" funded by the National Centre for Research and Development (grant agreement no. POIR.01.01.01-00-0857/19).

The project Innovative Liquid Micro Pulsed Plasma Thruster System for Nanosatellites (LμPPT) was funded by the European Commission (FP7 "LμPPT" project, No. 283279) and received support from the Foundation for Polish Science in years 2012-14.

The authors would like to acknowledge the company Semicon Sp. z o.o., specifically Piotr Ciszewski and Grzegorz Pasek, for their help with reflow soldering of the capacitor banks.

References

[1]Burton, R.L., and Turchi, P.J., „Pulsed plasma thruster", *J. Propul. Power*, Vol. 14, 1996, pp. 716–735.

[2]Levchenko, I., et al., "Space Micropropulsion Systems for Cubesats and Small Satellites: From Proximate Targets to Furthermost Frontiers," *Appl. Phys. Rev*. Vol. 5, 22 Apr. 2018, p. 011104 (1-36); URL: https://doi.org/10.1063/1.5007734

[3]Ling, W. Y. L., Zhang, S., Fu, H., Huang, M., Quansah, J., Liu X., Wang, N., "A brief review of alternative propellants and requirements for pulsed plasma thrusters in micropropulsion applications," *Chinese Journal of Aeronautics*, Vol. 33, Issue 12, 2020, pp. 2999-3010, https://doi.org/10.1016/j.cja.2020.03.024

[4]Lee, H. C., Lim, C. H., Woo, H. J., Goh, B. T., Chin, O. H., and Tou, T. Y., "Performance of pulsed plasma thruster at low discharge energy," *Plasma Sci. Technol*. Vol. 26 (2024) p. 045502(1-11), https://doi.org/10.1088/2058-6272/ad0d52

[5]Ciaralli, S., Coletti, M., and Gabriel, S.B., "Performance and lifetime testing of a pulsed plasma thruster for Cubesat applications," *Aerospace Science and Technology*, Vol. 47, December 2015, Pages 291-298, https://doi.org/10.1016/j.ast.2015.09.031

[6]Barral, S., Kurzyna, J., Rachubinski, H., Szelecka, A., Martin, R., Remirez, E., Ortiz, P., Alonso, J., Mabillard, Y., Bottinelli, S., Zaldivar, A., Rangsten, P., and Koppel, C. "First experimental characterization of a pulsed plasma thruster with non-volatile liquid propellant," *SPACE PROPULSION 2014*, Cologne, Germany, May 2014, paper 2980924.

[7]Barral, S., Kurzyna, J., Rachubinski, H., Szelecka, A., Daniłko, D., Martin, R., Remirez, E., Ortiz, P., Alonso, J., Mabillard, Y., Bottinelli, S., Zaldivar, A., Rangsten, P., and Koppel, C., "Time-of-flight spectrometry and performance of a pulsed plasma thruster with non-volatile propellant," *Jt. Conf. 30th Int. Symp. Space Technol. Sci., 34th Int. Electr. Propuls. Conf. and 6th Nano-satell. Symp*., IEPC-2015-141/ISTS-2015-b-141, Hyogo-Kobe, Japan, July 2015; https://electricrocket.org/IEPC/IEPC-2015-141_ISTS-2015-b-141.pdf

[8]ECSS, "Space product assurance — Data selection of space materials and processes," ECSS Q-70-71A (European Cooperation for Space Stadardization, Noordwijk, The Netherlands, 2004).

[9]Koizumi, H., Kakami, A., Furuta, Y., Komurasaki, K., and Arakawa, Y., „Liquid Propellant Pulsed Plasma Thruster," *28th International Electric Propulsion Conference*, IEPC-03-087, March 17-21, 2003, Toulouse, France.

[10]Scharlemann, C. A., "Investigation of Thrust Mechanisms in a Water Fed Pulsed Plasma Thruster," *PhD Dissertation*, 2003, The Ohio State University, Columbus, USA

[11]Kowalenkoy, V., "Revisiting the performance of a plasma armature railgun," *J. Phys. D: Appl. Phys*. Vol. 29, 1996, pp. 3050–3062.

[12]McDonald, K., "Capacitor-driven railgun: Magnetic fields doing work," 2017, http://kirkmcd.princeton.edu/examples/railgun.pdf.

[13]Jahn, R. G., *Physics of electric propulsion*, McGraw-Hill, New York, NY, 1968, Chapt. 9.G3

Copyright 2024 by the Electric Rocket Propulsion Society. All rights reserved.

[14]Peradzyński, Z., Makowski, K., Kurzyna, J., "Early stage of the discharge in ablative pulsed plasma thrusters," Plasma Sources Science and Technology, Vol. No. 2, Doi:, 10.1088/1361-6595/aaf95e

[15]Keidar, M., and Boyd, I. D., and Beilis, I. I., "Ionization and ablation phenomena in an ablative plasma accelerator," *J. Appl. Phys*. Vol. 96, No. 10, 15 Nov. 2004, pp. 5420-5428

[16]Guman, W. J., "Pulsed Plasma Technology in Microthrusters," *Air Force Aero Propulsion Laboratory*, AFAPL-TR-68-132, Air Force Systems Command, Wright-Patterson Air Force Base, Ohio 45433, Nov. 1968.

[17]Mikellides, P.G., Henrikson, E.M., and Rajagopalan, S. S., "Theoretical Formulation for the Performance of Rectangular, Breech-Fed Pulsed Plasma Thrusters," J. of Propulsion and Power, Vol. 35, No. 4, July–August 2019, pp. 811-818.

[18]Schönherr, T., Nawaz, A., Herdrich, G., Röser, H-P., and Auweter-Kurtz, M., "Influence of Electrode Shape on Performance of Pulsed Magnetoplasmadynamic Thruster SIMP-LEX," *Journal of Propulsion and Power*, Vol. 25, No. 2, March–April 2009.

[19]"Rideshare Payload User's Guide", Version 9 -December 2023, Space Exploration Technologies Corp. (SpaceX) https://storage.googleapis.com/rideshare-static/Rideshare_Payload_Users_Guide.pdf

[20]Kurzyna, J. Jakubczak, M., Szelecka, A. and Dannenmayer, K., "Performance tests of IPPLM's krypton Hall thruster," *Laser and Particle Beams*, Vol. 36, Issue 1, March 2018, pp. 105–114, https://doi.org/10.1017/S0263034618000046

[21]Kurzyna, J., Jakubczak, M., Szelecka, A., and Riazantsev, A., "Preliminary Tests of HIKHET Laboratory Model at IFPiLM," *36th International Electric Propulsion Conference*, IEPC-2019-591, Vienna, Austria, September 15-20, 2019

[22]Riazantsev, A., Jakubczak, M., Cichorek, O., and Kurzyna, J., „Side and Front Imaging of Plasma Discharge Evolution in an Ablative Pulsed Plasma Thruster Operated with Solid and Liquid Propellants," to be published.

Copyright 2024 by the Electric Rocket Propulsion Society. All rights reserved.